

*NUCLEAR MAGNETIC RESONANCE OF  $\beta$ -ACTIVE  $\text{Li}^8$  NUCLEI FORMED BY CAPTURE  
OF POLARIZED NEUTRONS IN  $\text{LiF}$  SINGLE CRYSTALS*

M. I. BULGAKOV, A. D. GUL'KO, Yu. A. ORATOVSKIĬ and S. S. TROSTIN

Institute of Theoretical and Experimental Physics

Submitted February 11, 1971

Zh. Eksp. Teor. Fiz. 61, 667–677 (August, 1971)

Measurements were made of the room-temperature profile of the NMR line of polarized  $\beta$ -active  $\text{Li}^8$  nuclei formed by the capture of polarized thermal neutrons. The investigation was carried out on three  $\text{LiF}$  single crystals, oriented with their (100), (110), and (111) planes at right-angles to the magnetic field, and on two powder samples of  $\text{LiF}$  and  $\text{Li}^7\text{F}$  (with a reduced concentration of  $\text{Li}^6$ ). The line profile was investigated by suppressing, with a radio-frequency field  $H_1$ , the angular anisotropy of  $\beta$  rays emitted by the polarized  $\text{Li}^8$  nuclei. A theoretical calculation of the line profile was carried out assuming a dipole-dipole interaction in a rigid lattice. The second moments of the line profile were calculated. A comparison with the experimental results demonstrated that the internal local fields at the  $\text{Li}^8$  nuclei had a Gaussian distribution and only wings were subject to a Lorentzian deviation ( $\sim 10^{-2}$  of the maximum value). Lattice defects generated by the  $\gamma$ -ray recoil of the  $\text{Li}^8$  nuclei did not affect significantly the resonance line profile.

## INTRODUCTION

INVESTIGATIONS of polarized  $\beta$ -active nuclei are attracting increasing interest and finding increasing applications.<sup>[1-7]</sup> First, this is due to the relative ease of the formation of strongly polarized systems of  $\beta$ -active nuclei in nuclear reactions (the degree of polarization is usually 10–40%). Secondly, the polarization can be measured quite easily (in spite of the small absolute numbers of polarized nuclei) by determining the angular anisotropy of the  $\beta$  rays emitted by polarized nuclei. This method has been used, in conjunction with the NMR method, to determine the spins, magnetic moments, and electric quadrupole moments of several  $\beta$ -active nuclei.<sup>[2-6]</sup> Thirdly, polarized  $\beta$ -active nuclei in a crystal lattice act as microprobes. A study of the profile of the NMR lines of such nuclei gives information on the distribution of internal crystal fields, on the positions of  $\beta$ -active nuclei in the lattice, and on the nature of their interaction with the environment.

Interactions of a  $\beta$ -active nucleus with the surrounding unpolarized nuclei in a target differ in several respects from the interactions of the corresponding stable isotopes. First, a system of polarized  $\beta$ -active nuclei forms a highly dilute solution in a large number of unpolarized stable nuclei (the concentration of the polarized nuclei is usually  $\sim 10^{-15}$ – $10^{-19}$ ). Secondly, the  $g$  factor of a  $\beta$ -active nucleus is usually quite different from the  $g$  factors of the surrounding stable nuclei in the target. Therefore, the spin-spin interaction between the two types of nuclei is much weaker than usual. Moreover, the recoil energy of a  $\beta$ -active nucleus formed by a nuclear reaction may be so high that the nucleus is knocked out of its regular lattice site. This effect may give rise to a large number of defects around a  $\beta$ -active nucleus which has come to rest.

All these features of the interaction between the nuclei and their environment may affect the NMR line profile and the relaxation mechanism.

An interesting feature of the NMR method described in the present paper is the fact that the resonance absorption may be observed also for large amplitudes of the radio-frequency field whereas in the usual studies of the stable nuclei by the NMR method such absorption cannot be observed because of the saturation factor. The use of large amplitudes makes it possible to determine the NMR line profile very far from the resonance frequency.

In the present investigation we generated polarized  $\beta$ -active nuclei by means of the  $(n, \gamma)$  reaction in which polarized thermal neutrons were used. We studied the NMR of  $\beta$ -active  $\text{Li}^8$  nuclei in  $\text{LiF}$  single crystals at room temperature.

## EXPECTED DISTRIBUTION OF LOCAL FIELDS AND CALCULATION OF MOMENTS OF LINE PROFILE

When a thermal neutron is captured by  $\text{Li}^7$ , the resultant excited  $\text{Li}^8$  nucleus remains at the original lattice site because the average energy for displacement of an atom from a site is 25 eV.<sup>[7]</sup> Subsequently, the  $\text{Li}^8$  nucleus undergoes a transition from the excited to the ground state, emits a  $\gamma$  quantum, and experiences a recoil. The recoil energy is  $\sim 300$  eV so that an ion containing a  $\beta$ -active nucleus is displaced from its lattice site. During subsequent deceleration (lasting about  $10^{-13}$  sec) the displaced ion knocks out neighboring ions from their sites. This may give rise to defects (vacancies and atom pairs) near the point where the  $\text{Li}^8$  nucleus comes to rest. Such a disturbance of the crystal lattice increases the local fields and, consequently, alters the NMR line profile compared with the profile of an  $\text{Li}^8$  nucleus at a site in a perfect lattice. If there is significant annealing of the defects (this depends on temperature), we may expect the line profile of the NMR line to approach that expected for a defect-free crystal.

We shall calculate theoretically the line profile for an  $\text{LiF}$  sample on the assumption that  $\beta$ -active  $\text{Li}^8$  nuclei

occupy the normal positions of lithium nuclei in the LiF lattice. We shall use the theory of the line profile for a rigid lattice.<sup>[8,9]</sup>

We have to consider three types of spin and take into account the fact that the  $g$  factor of the  $\beta$ -active  $\text{Li}^8$  nuclei differs strongly from the  $g$  factors of the surrounding  $\text{Li}^7$  and  $\text{F}^{19}$  nuclei (the  $\text{Li}^8$  nuclei are separated by very large distances of  $\sim 10^6$  Å). Therefore, we must exclude the spin-flipping term from the Hamiltonian of the dipole-dipole interaction and retain only the static component. Then, the second moment of the NMR line profile of the  $\text{Li}^8$  nuclei is obtained in the form:<sup>[8]</sup>

$$M_2 = \frac{1}{3} I'(I' + 1) \frac{1}{\hbar^2} \sum_k G_{jk}^2, \quad (1)$$

$$G_{jk} = g_I g' \mu^2 r_{jk}^{-3} (1 - 3\gamma_{jk}^2), \quad (1a)$$

where  $g_I$  is the  $g$  factor of  $\text{Li}^8$ ;  $g'$  and  $I'$  are, respectively, the  $g$  factor and the spin of the surrounding nuclei;  $r_{jk}$  is the radius vector directed from the  $j$ -th  $\text{Li}^8$  nucleus to the  $k$ -th nucleus;  $\gamma_{jk} = \cos \theta_{jk}$ ;  $\theta_{jk}$  is the angle between  $r_{jk}$  and the direction of the external static magnetic field  $H_0$ ;  $\mu_k$  is the nuclear magneton. The summation is carried out over all the surrounding nuclei.

In the case of a powder, when the orientation of the individual grains is distributed uniformly over a sphere, the expression for  $M_2$  includes the average value  $(1 - 3\gamma_{jk}^2)^2$ . In this case the formula for  $M_2$  assumes the form

$$M_2 = \frac{4}{15} \frac{g_I^2 g'^2 \mu_k^4}{\hbar^2} I'(I' + 1) \sum_k r_{jk}^{-6}. \quad (2)$$

In the case of a cubic single crystal the sums  $\Sigma \gamma_{jk}^2$  and  $\Sigma \gamma_{jk}^4$  occur in the expression (1) for the second moment. A calculation of these sums gives the formulas:<sup>[8]</sup>

$$M_2 = \frac{1}{6\hbar^2} g_I^2 g'^2 \mu_k^4 I'(I' + 1) [a + b(\lambda_1^4 + \lambda_2^4 + \lambda_3^4)], \quad (3)$$

where

$$a = \sum_k r_{jk}^{-6} [7 - 9(\xi_{jk}^4 + \eta_{jk}^4 + \zeta_{jk}^4)], \quad (3a)$$

$$b = \sum_k r_{jk}^{-6} [-9 + 15(\xi_{jk}^4 + \eta_{jk}^4 + \zeta_{jk}^4)], \quad (3b)$$

where  $\xi_{jk}$ ,  $\eta_{jk}$ ,  $\zeta_{jk}$  and  $\lambda_1$ ,  $\lambda_2$ ,  $\lambda_3$  are, respectively, the direction cosines of the radius vector  $r_{jk}$  and of the axis coinciding with the direction of  $H_0$ , both of them referred to the principal axes system of the cubic lattice.

The values of  $M_2$  calculated by means of Eqs. (2) and (3) are found to be 9/4 times smaller than those for a single crystal with one type of nucleus. This is due to the absence of the spin-flipping terms in the Hamiltonian of the dipole-dipole interaction.

If it is assumed that a  $\beta$ -active nucleus occupies a regular lattice site, the crystal structure of LiF in relation to this nucleus can be represented by a sequence of spherical layers of  $\text{Li}^7$  and of  $\text{F}^{19}$  atoms. An important point to note is that the  $\text{Li}^7$  and  $\text{F}^{19}$  atoms are not mixed in a layer with a given value of  $r_{jk}$ . Then, the

summation over all the surrounding nuclei in Eqs. (3a) and (3b) can be separated into summation over layers. In our case it is sufficient to consider the first seven layers.

The influence of the  $\text{Li}^6$  nuclei must be allowed for in calculations of  $M_2$  for natural samples of LiF, which consist of 92.6%  $\text{Li}^7$  and 7.4%  $\text{Li}^6$ . In this case the contribution of the lithium nuclei to the second moment is of the form

$$M_2(\text{Li}) = M_2\rho + M_2'\rho', \quad (4)$$

where  $M_2$  and  $M_2'$  are, respectively, the contributions of  $\text{Li}^7$  and  $\text{Li}^6$  to the second moment of the line profile, as calculated by means of Eqs. (2) or (3);  $\rho$  and  $\rho'$  are the corresponding isotopic concentrations of  $\text{Li}^7$  and  $\text{Li}^6$  in a given sample.<sup>1)</sup>

The second moments calculated in this way for various samples of LiF are given in Table I. It is evident from the data given in the table that the correction for the presence of  $\text{Li}^6$  is small.

However, the knowledge of the second moment is not sufficient for deduction of the line profile. An important characteristic of the line profile is the ratio of its fourth moment to the square of its second moment:  $M_4/M_2^2$ . For example, for the Gaussian profile this ratio is  $M_4/M_2^2 = 3$ . If the line profile deviates toward the Lorentzian curve, this ratio is larger than 3 and when it deviates toward a rectangular shape, the ratio is less than 3. It is quite difficult to calculate theoretically the value of  $M_4$  for the many-spin system we are considering and we can only make some qualitative comments about the possible line profile. An estimate obtained following the procedure outlined in<sup>[9]</sup> gives  $M_4/M_2^2$  equal to a few tens. This means that we should expect a considerable quasi-Lorentzian narrowing of the NMR line. The physical reason for this is the mutual reversal of spins in the system of the surrounding nuclei. The magnitude of this effect may be different for samples oriented in different ways with respect to the static magnetic field. The largest effect is to be expected for a sample whose [100] crystallographic axis is oriented along the  $H_0$  field and the smallest effect for a sample with its [111] axis along  $H_0$ . This is due to the fact that the interaction of the  $\text{Li}^8$  and  $\text{F}^{19}$  nuclei is strongest when  $H_0$  is aligned along the [100] axis and weakest when  $H_0$  is oriented along the [111] axis.

#### METHOD FOR DETERMINATION OF THE NMR LINE-PROFILE FUNCTION OF POLARIZED $\beta$ -ACTIVE NUCLEI

The angular distribution of  $\beta$  rays emitted by polarized nuclei is known to be anisotropic. However, the anisotropy can be destroyed by applying a radio-frequency magnetic field of Larmor frequency. The dependence of the  $0-\pi$  asymmetry of  $\beta$  decay of polarized radioactive nuclei,  $\epsilon_{\nu}$ , on the frequency of the applied radio-frequency field,  $\nu$ , is of the form:<sup>[1]</sup>

<sup>1)</sup> Although the  $g$  factor of  $\text{Li}^6$  (0.8233) is close to the  $g$  factor of  $\text{Li}^8$  (0.8265), the overlap of the resonance lines of these nuclei is small ( $\sim 1\%$ ) in the static field  $H_0 = 3000$  Oe employed in our investigation. Therefore,  $M_2'$  can be calculated ignoring the spin-flipping term and making allowance solely for the static part of the interaction.

Sample	$A'_0$ , kHz	$M_2$ , theor, kHz <sup>2</sup>	$M_2$ , exp, kHz <sup>2</sup>	$M_4$ , exp, kHz <sup>4</sup>	$M_4/M_2^2$ (exp.)	$\Delta H_{loc, exp}$ Oe	$\Delta H_{loc, theor} = 1.67 / (2M_2, theor)^{1/2}$ , Oe
LiF	0.444 ± 0.011	13.70 (13.76) *	14.42 ± 0.38	715 ± 24	3.4	13.6 ± 0.18	~13.8
[100] LiF	0.432 ± 0.011	4.86 (4.95) *	5.44 ± 0.19	151 ± 8	5.1	8.2 ± 0.14	8.3
[110] LiF	0.413 ± 0.011	1.944 (2.014) *	2.59 ± 0.13	50 ± 5	7.4	5.1 ± 0.13	5.2
[111] LiF	0.418 ± 0.015	6.709 (6.713) *	6.72 ± 0.34	207 ± 15	4.6	8.6 ± 0.22	9.6
powder Li <sup>7</sup> F	0.424 ± 0.014	6.713	6.19 ± 0.33	194 ± 15	5.1	8.6 ± 0.23	9.6

\*Without allowance for the presence of Li<sup>6</sup>.

$$\epsilon_v = \frac{\epsilon_0 \lambda^2}{[\lambda + T_1^{-1} + 1/2 b \gamma^2 H_1^2 f(\nu)]^2} \times \frac{1 - \exp\{-[\lambda + T_1^{-1} + 1/2 b \gamma^2 H_1^2 f(\nu)] t_0\}}{1 - \exp(-\lambda t_0)} \times \frac{1 - \exp\{-[\lambda + T_1^{-1} + 1/2 b \gamma^2 H_1^2 f(\nu)] \Delta t\}}{1 - \exp(-\lambda \Delta t)} \times \exp\{-[T_1^{-1} + 1/2 b \gamma^2 H_1^2 f(\nu)] t\}. \quad (5)$$

Here,  $\epsilon_0$  is the decay asymmetry at the moment of formation of polarized  $\beta$ -active nuclei;  $\lambda$  is the decay constant;  $T_1$  is the relaxation time of the system of polarized  $\beta$ -active nuclei;  $t_0$  is the duration of irradiation of a sample with polarized neutrons;  $\Delta t$  is the time taken to measure the asymmetry;  $t$  is the time from the end of irradiation to the beginning of measurements;  $\gamma$  is the gyromagnetic ratio of the polarized nuclei;  $b$  is a coefficient which depends on the nuclear spin and on the law of occupancy of levels in the polarized system;  $H_1$  is the amplitude of the rotating radio-frequency field;  $f(\nu)$  is the normalized function representing the resonance line profile, determined by the distribution of internal crystal fields at the  $\beta$ -active nuclei.

It is practically impossible to use Eq. (5) directly in determination of the profile function  $f(\nu)$  because the absolute value of  $H_1$  must be known. Therefore, we shall use a different function  $\kappa(\nu)$ :

$$\kappa(\nu) = \frac{b \gamma^2 H_1^2}{2(\lambda + T_1^{-1})} f(\nu). \quad (6)$$

This function represents the radio-frequency absorption during the lifetime of a nucleus in the polarized state. Then, assuming that (as in our experiments)  $t = 0$  and  $\tilde{\lambda} = \lambda + T_1^{-1}$ , we find from Eq. (5) that

$$\frac{\epsilon_v}{\epsilon_\infty} = \frac{1}{(1 + \kappa)^2} \frac{1 - \exp[-\tilde{\lambda}(1 + \kappa)t_0]}{1 - \exp(-\tilde{\lambda}t_0)} \frac{1 - \exp[-\tilde{\lambda}(1 + \kappa)\Delta t]}{1 - \exp(-\tilde{\lambda}\Delta t)}, \quad (7)$$

where  $\epsilon_\infty$  is the asymmetry of the  $\beta$  decay far from the resonance frequency. The value of  $\epsilon_v/\epsilon_\infty$  is found experimentally and the transcendental equation (7) is solved for  $\kappa$  graphically if the values of  $\tilde{\lambda}$ ,  $t_0$ , and  $\Delta t$  are known.

We shall consider two ways of calculating the line profile function  $f(\nu)$ .

In the first case, when the relaxation time  $T_1$  is known, the quantity  $\tilde{\lambda}$  is determined and Eq. (7) is used to find  $\kappa$ . Equation (6) is modified by the substitution

$$A \equiv \frac{b \gamma^2 H_1^2}{2(\lambda + T_1^{-1})}, \quad (8)$$

which gives the following relationship for the line profile function:

$$f(\nu) = \kappa(\nu) / A. \quad (9)$$

The value of  $A$  can be found by graphical integration of the experimentally determined curve  $\kappa(\nu)$ :

$$\int_{-\infty}^{+\infty} \kappa(\nu) d\nu = \frac{b \gamma^2 H_1^2}{2(\lambda + T_1^{-1})} \int_{-\infty}^{+\infty} f(\nu) d\nu = \frac{b \gamma^2 H_1^2}{2(\lambda + T_1^{-1})} = A, \quad (10)$$

since  $\int_{-\infty}^{+\infty} f(\nu) d\nu = 1$  because of normalization of the profile function.

Thus, the use of  $\kappa$  makes it possible to determine the profile function  $f(\nu)$  without the knowledge of the radio-frequency field  $H_1$  and of the parameters  $b$  and  $\gamma$ .

In the second case, when the relaxation time  $T_1$  is not known, the solution of Eq. (7) is found in the linear approximation:

$$\kappa = \kappa' / a \quad (a \geq 1), \quad (11)$$

where  $\kappa'$  is the solution of Eq. (7) for  $\tilde{\lambda} = \lambda$ . The coefficient  $a$  depends on the relaxation time  $T_1$ : the lower the value of  $T_1$ , the higher is the value of this coefficient. In principle, the relationship between  $\kappa'$  and  $\kappa$  is nonlinear, i.e., the coefficient  $a$  depends on  $\kappa'$ . However, in a fairly narrow range of  $\kappa'(\nu)$  the nonlinearity can be ignored. In the specific case of Li<sup>6</sup> a numerical calculation shows that when  $\kappa'$  is varied between 0.05 and 2, which corresponds to  $\epsilon_v/\epsilon_\infty$  from 0.9 to 0.1, the value of  $a$  varies by only 1%. This variation lies within the limits of the experimental error in our measurements.

Thus, instead of Eqs. (9) and (10) we obtain

$$f(\nu) = \kappa'(\nu) / A', \quad (12)$$

$$\int_{-\infty}^{+\infty} \kappa'(\nu) d\nu = a \frac{b \gamma^2 H_1^2}{2(\lambda + T_1^{-1})} = A' = aA. \quad (13)$$

Here,  $A'$  is the area under the experimentally determined dependence  $\kappa'(\nu)$ , which can be found graphically. We can see that, once again, the use of the expression for  $\kappa$  makes it possible to find the profile function  $f(\nu)$  without the knowledge of the parameters  $b$ ,  $\gamma$ ,  $H_1$ , and even  $T_1$ .

It is worth noting that Eq. (13) can be used—in principle—to find the relaxation time  $T_1$ . This can be done as follows. We can measure the area under the  $\kappa'$  curve and, knowing the values of  $b$ ,  $\gamma$ , and  $H_1$ , we can find the function  $a(T_1)/[1 + (1/\lambda T_1)]$ . The calculated dependence of this function on  $T_1$  yields a value of  $T_1$ .

In the presence of one type of  $\beta$ -active nuclei the knowledge of the relaxation time  $T_{1,0}$  for a particular compound can be used, in conjunction with the measured

areas  $A'$  (found for a constant amplitude of  $H_1$ ), to determine  $T_1$  of the same nuclei in other compounds:

$$\frac{A'}{A_0'} = \frac{a(T_1)(1 + \tau/T_{1,0})}{(1 + \tau/T_1)a(T_{1,0})}, \quad (14)$$

where  $\tau = 1/\lambda$  is the lifetime of the  $\beta$ -active nuclei. If  $T_{1,0} \gg \tau$ , it follows that  $a(T_{1,0}) = 1$  and  $T_1$  is found from the expression

$$\frac{A'}{A_0'} = \frac{a(T_1)}{1 + \tau/T_1}. \quad (15)$$

It follows from Eqs. (6) and (7) that the experimentally determined profile of the NMR line of polarized  $\beta$ -active nuclei depends on the amplitude of the radio-frequency field  $H_1$ . Moreover, as pointed out in<sup>[1]</sup>, Eq. (5) is valid in fields  $H_1$  in which the asymmetry decreases approximately to  $0.5\epsilon_\infty$  (this is a consequence of the application of the perturbation theory). The upper limit for the field  $H_1$  in which the relationships deduced are still valid can be found experimentally by measuring the function  $\kappa$  for different amplitudes of  $H_1$ . Then, the "reduced" distribution function

$$\kappa_0' = \kappa'(H_1/H_{1,0})^{-2} \quad (16)$$

should be independent of  $H_1$ . In this expression  $H_{1,0}$  is some sufficiently small amplitude of the radio-frequency field and  $H_1$  and  $\kappa'$  are, respectively, the given amplitude of the radio-frequency field and the absorption function corresponding to this field.

It also follows from Eqs. (6) and (7) that the function  $f(\nu)$  can be determined at frequencies very far from the resonance point. The line profile near the resonance frequency is usually determined employing weak fields  $H_1$ . Then, far from the resonance point where  $f(\nu)$  is small, the values of  $H_1^2 f(\nu)$  and, consequently, of  $\kappa$  are small. Therefore, the change in the asymmetry  $\epsilon_\nu$  will be small. The application of a sufficiently strong field  $H_1$  can make the values of  $H_1^2 f(\nu)$  and  $\kappa$  so large that the change in the asymmetry  $\epsilon_\nu$  will be considerable ( $\epsilon_\nu \sim 0.5\epsilon_\infty$ ). In this way we can measure very small values of  $f(\nu)$ .

## MEASUREMENTS AND RESULTS

The apparatus and the experimental procedure employed in the determination of the  $0-\pi$  asymmetry of the  $\beta$  decay of polarized nuclei, formed by the capture of polarized thermal neutrons, were described in<sup>[1,2]</sup>. The measurements reported in the present paper were carried out using automatic equipment which included time and radiation intensity monitoring systems. This made it possible to determine the asymmetry simultaneously in both counting channels or in each channel separately.

The measurements of the NMR of the  $\text{Li}^8$  nuclei ( $T_{1/2} = 0.85$  sec) were carried out on five samples of LiF: four of these samples contained the natural proportions of the  $\text{Li}^7$  and  $\text{Li}^6$  isotopes and one sample contained nearly 100% of the  $\text{Li}^7$  isotope. These samples were in the form of plates 2 mm thick and of  $40 \times 40$  mm<sup>2</sup> area. Three LiF samples were single crystals cut in such a way that their (100), (110), and (111) planes were parallel to the large surface. The fourth sample of LiF and the  $\text{Li}^7\text{F}$  sample were polycrystalline powders prepared by crushing without subsequent annealing. All these LiF samples originated from

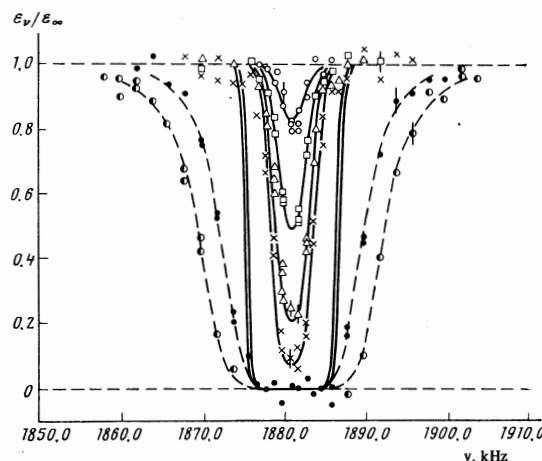


FIG. 1. Frequency dependence of the asymmetry of the  $\beta$  decay of  $\text{Li}^8$  nuclei in a single crystal of LiF.  $H_0 \parallel [111]$ ,  $H_0 = 2984.9$  Oe. (O)  $2H_1 = 0.013$  Oe; (□) 0.025 Oe; (Δ) 0.04 Oe; (X) 0.06 Oe; (●) 0.94 Oe; (●) 1.75 Oe. The continuous curves represent theoretical calculations based on the assumption of a Gaussian line profile  $f(\nu)$  with  $\sigma = \sqrt{2M_2}$ ,  $\text{theor} = 1.96$  kHz.

the same single crystal. The samples were placed at the center of an electromagnet with their large faces perpendicular to the magnetic field (within 2%). The irradiation time  $t_0$  and the measuring time  $\Delta t$  were, respectively, 3.73 and 4 sec.

The  $0-\pi$  asymmetry of the  $\beta$  decay of  $\text{Li}^8$  was found by subtracting the asymmetry of the  $\beta$  decay of  $\text{F}^{20}$  (formed in the LiF samples) from the experimentally determined curves. The asymmetry of the  $\text{F}^{20}$  nuclei was taken to be the asymmetry which remained after total depolarization of the  $\text{Li}^8$  nuclei by the application of a strong radio-frequency field.<sup>[1,2]</sup> The background radiation was found to have no influence on the ratio  $\epsilon_\nu/\epsilon_\infty$  and, consequently, on the NMR line profile.

Figure 1 shows typical dependences of  $\epsilon_\nu/\epsilon_\infty$  for  $\text{Li}^8$  on the frequency and amplitude of the field  $H_1$ . The functions  $\kappa_0'$  were calculated from the values of  $\epsilon_\nu/\epsilon_\infty$  by means of Eqs. (7) and (16). These functions were reduced to the same value of  $H_{1,0}$  for all five samples. Next, we found the areas  $A_0'$  under the  $\kappa_0'$  curves and we applied Eqs. (12) and (13) to determine the profile function  $f(\nu)$ . The second and fourth moments of the resonance line profiles were found from the formulas

$$M_n = \int_{-\infty}^{+\infty} (\nu - \nu_0)^n \kappa_0'(\nu) d\nu / \int_{-\infty}^{+\infty} \kappa_0'(\nu) d\nu = \int_{-\infty}^{+\infty} (\nu - \nu_0)^n f(\nu) d\nu. \quad (17)$$

The results obtained are presented in Table I and in Figs. 2-4.

The areas  $A_0'$  were found to be the same for all the samples (this was true within the limits of the experimental error). Hence, using Eq. (14) we concluded that the relaxation times  $T_1$  of the  $\text{Li}^8$  nuclei were the same in all five samples. The known values of  $H_{1,0}$  substituted into Eq. (13) indicated that  $T_1 \gtrsim 15$  sec. A more accurate value of  $T_1$  would be obtained if we were to increase the precision of the measurement of the radio-frequency field  $H_{1,0}$ .

Figure 2 shows the results of measurements of the function  $f(\nu)$  for a sample subjected to a static field  $H_0 \parallel [111]$  and radio-frequency fields of various ampli-

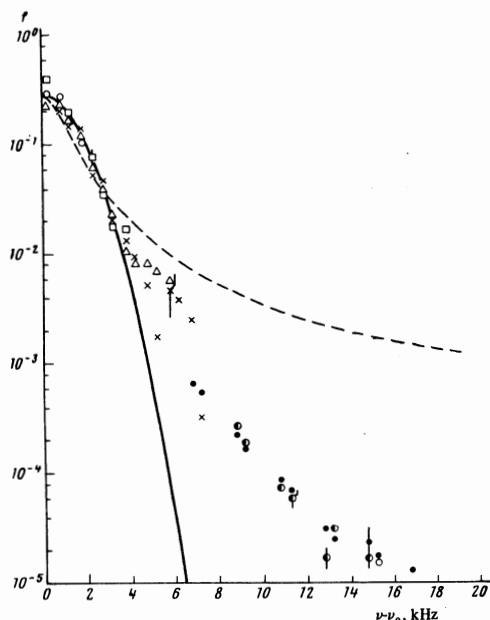


FIG. 2. Line profile  $f(\nu)$  of  $\text{Li}^8$  nuclei in a single crystal of  $\text{LiF}$ .  $H_0 \parallel [111]$ . The experimental points have the same meaning as in Fig. 1. The continuous curve is a Gaussian profile with  $\sigma = 1.96$  kHz; the dashed curve is the Lorentzian profile.

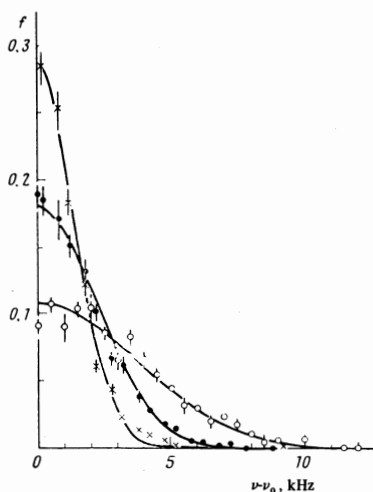


FIG. 3. Top part of the function  $f(\nu)$  for  $\text{Li}^8$  nuclei in single crystals of  $\text{LiF}$ . The experimental points represent averages for different amplitudes of the radio-frequency field. (○)  $H_0 \parallel [100]$ ; (●)  $H_0 \parallel [110]$ ; (×)  $H_0 \parallel [111]$ . The continuous curves are Gaussian profiles with  $\sigma = \sqrt{2M_2}$ , theor equal to 5.24 kHz for  $H_0 \parallel [100]$ , 3.12 kHz for  $H_0 \parallel [110]$ , and 1.96 kHz for  $H_0 \parallel [111]$ .

tudes. The logarithmic scale was selected in order to show the line profile  $f(\nu)$  far from resonance. The results obtained indicated that the values of  $f(\nu)$  obtained using fields  $H_1$  of different amplitudes were identical (within the limits of the experimental error) if the  $H_1$  amplitudes were such that the ratio  $\epsilon_\nu/\epsilon_\infty$  was not less than 0.1. This defined the range of validity of the analytic expression (5). Similar results were obtained for the other four samples.

Figures 3 and 4 give the results of measurements of the function  $f(\nu)$  for all five samples. These results

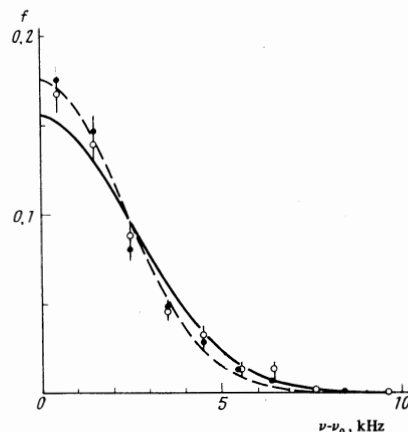


FIG. 4. Top part of the function  $f(\nu)$  for  $\text{Li}^8$  nuclei in polycrystalline samples of  $\text{LiF}$  and  $\text{Li}^7\text{F}$ . The continuous curve is a Gaussian profile with  $\sigma = 3.64$  kHz; the dashed curve is a Gaussian profile with  $\sigma = 3.2$  kHz. (○)  $\text{LiF}$  powder; (●)  $\text{Li}^7\text{F}$  powder.

were the averages obtained by using different amplitudes of the radio-frequency field.

The theoretical values of the second moments of the line profile were employed to plot the profile functions  $f(\nu)$  in the form of Gaussian and Lorentzian curves. The Lorentzian shape differed from the experimental curves both far from and close to the resonance frequency. In the case of single crystals the Gaussian shape was in good agreement with the experimental curve in the main part of the resonance line up to  $f \sim 10^{-2} f_{\text{max}}$  (Fig. 3).

The experimental  $f(\nu)$  curves obtained for the  $\text{LiF}$  and  $\text{Li}^7\text{F}$  powders were identical (within the limits of the experimental error). However, the calculated Gaussian curves with a theoretical half-width  $\sigma = \sqrt{2M_2}$ , theor = 3.64 kHz were in poorer agreement with the experimental curves near the resonance frequency. The best agreement was obtained for a Gaussian curve with  $\sigma = 3.2$  kHz (Fig. 4).

Far from the resonance frequency, in the range  $f \lesssim 10^{-2} f_{\text{max}}$ , the experimental points obtained for all the samples deviated from the calculated Gaussian curve toward the Lorentzian shape (Fig. 2). This quasi-Lorentzian nature of the  $f(\nu)$  curves was in agreement with the experimental values of the ratio  $M_4/M_2^2$ , which were more than 3 for all five samples (Table I).

Thus, a comparison of the experimental  $f(\nu)$  curves with the theoretical profile functions yielded the following conclusions. The distribution of the internal local fields at the  $\text{Li}^8$  nuclei, formed as a result of irradiation of  $\text{LiF}$  with thermal neutrons, were of the Gaussian shape with wings deviating toward the Lorentzian profile. The internal fields  $\Delta H_{\text{LOC}}$ , assumed to be represented by the widths of the  $f(\nu)$  curves at mid-amplitude, were in good agreement with the width of a Gaussian curve calculated on the basis of a model postulating a dipole-dipole interaction in a rigid lattice. The narrowing of the NMR lines of the powders, compared with the theoretical profiles, was evidently not accidental because it was observed for the  $\text{LiF}$  and  $\text{Li}^7\text{F}$  samples. This narrowing was probably due to residual stresses which were generated during the preparation of the powder samples (during grinding of the single crystal).

The experimental values of the second moments of the line profile obtained for single crystals exceeded the theoretical values by an average of  $\Delta M_2 = 0.65 \pm 0.1$  kHz<sup>2</sup>. Since the influence of the spin-lattice relaxation time  $T_1$  and of the inhomogeneity of the field  $H_0$  on the line profile could be ignored, we attributed this effect to the interaction between the  $\beta$ -active nuclei and the lattice defects, including those which resulted from the  $\gamma$ -recoil of the  $\text{Li}^8$  nuclei. The experimental values of the second moments of the line profile for the powders were in better agreement with the theoretical values. This was probably the consequence of the narrowing of the top part of the  $f(\nu)$  curve. A confirmation of this conclusion would require a study of annealed powders.

An analysis of the line profile exhibited by different samples of LiF indicated that the profile was in good agreement with the dipole-dipole interaction theory. Moreover, it confirmed the occurrence of annealing of the radiation defects at room temperature as a result of which those  $\beta$ -active nuclei which suffered  $\gamma$ -recoil re-occupied the regular sites in the LiF lattice.

<sup>1</sup>A. D. Gul'ko, S. S. Trostin, and A. Khudoklin, Zh. Eksp. Teor. Fiz. 52, 1504 (1967) [Sov. Phys.-JETP 25, 998 (1967)].

<sup>2</sup>A. D. Gul'ko, S. S. Trostin, and A. Khudoklin, Yad. Fiz. 6, 657 (1967) [Sov. J. Nucl. Phys. 6, 477 (1968)].

<sup>3</sup>H. Rauch, Z. Phys. 197, 373 (1966).

<sup>4</sup>K. Sugimoto, A. Mizobuchi, K. Nakai, and K. Matuda, J. Phys. Soc. Jap. 21, 213 (1966); K. Sugimoto, K. Nakai, K. Matuda, and T. Minamisono, Phys. Lett. 25B, 130 (1967); K. Sugimoto, A. Mizobuchi, K. Matuda, and T. Minamisono, Phys. Lett. 31B, 520 (1970).

<sup>5</sup>H. Ackermann, D. Dubbers, J. Mertens, A. Winnacker, and P. von Blanckenhagen, Phys. Lett. 29B, 485 (1969).

<sup>6</sup>L. Pfeiffer, J. C. Wells Jr. and L. Madansky, In: E. Matthias and D. A. Shirley (eds.), Hyperfine Structure and Nuclear Radiations (Proc. Intern. Conf. on Hyperfine Interactions Detected by Nuclear Radiation, Pacific Grove, Calif., 1967), North-Holland, Amsterdam, 1968, p. 871.

<sup>7</sup>B. T. Kelly, Irradiation Damage to Solids, Pergamon Press, Oxford, 1966 (Russ. Transl., Atomizdat, M., 1970).

<sup>8</sup>A. Lösche, Kerninduktion, Deutsche Verlag den Wissenschaften, Berlin, 1957 (Russ. Transl., IIL, M., 1963).

<sup>9</sup>A. Abragam, The Principles of Nuclear Magnetism, Clarendon Press, Oxford, 1961 (Russ. Transl. IIL, M., 1963).